AMSE JOURNALS –2015-Series: Modelling B; Vol. 84; N° 2; pp 105-124
Submitted April 2015; Revised Sept. 21, 2015; Accepted Nov. 30, 2015

Ionized Fluid Flow on Impulsive Vertical Porous Plate with Inclined Magnetic Field

*Tanvir Ahmed, **Md. Mahmud Alam

Mathematics Discipline, Science, Engineering and Technology School,
Khulna University, Khulna-9208, Bangladesh
(*tanvir1989bd@gmail.com, **alam_mahmud2000@yahoo.com)

Abstract

The ionized fluid flow on impulsive vertical plate in porous media in the presence of internal heat generation with chemical reaction, thermal radiation and inclined magnetic field has been studied numerically for small magnetic Reynolds number. To obtain the non-dimensional non-similar momentum, energy and concentration equations, usual non-dimensional variables have been used. The obtained non-dimensional equations have been solved by explicit finite difference method as well as implicit finite difference method. The effects of the various parameters entering into the problem on the velocity, temperature and concentration profiles are shown graphically. Finally, a qualitative comparison with previous work is shown in tabular form.

Key words

Ionized fluid, inclined magnetic field, chemical reaction, finite difference method

1. Introduction

The ionized fluid flow on MHD boundary layer flow has become important in several industrial, scientific and engineering fields. For ionized fluid two distinct effects have been considered by Cowling [1]. First effect, electric currents can flow in an ionized fluid because of relative diffusion of the ionized gas and electrons, due to agencies of electric forces. The second effect depends wholly on the magnetic field. The convection flow is often encountered in nuclear reactors or in the study of planets and stars. In this flow the phenomenon of mass transfer is also very common in the theories of stellar structure. The studies of MHD incompressible viscous flows with Hall currents have grown considerably because of its engineering applications to the problems

of Hall accelerators, MHD generators, constructions of turbines and centrifugal machines, as well as flight magnetohydrodynamics. From the above point of applications, the effects of Hall currents on free convective flow through a porous medium bounded by an infinite vertical plate have been studied by Ram [2], when a strong magnetic field is imposed in a direction which is perpendicular to the free stream and makes an angle to the vertical direction. The Hall effects on an unsteady MHD free convective heat and mass transfer flow through a porous medium near an infinite vertical porous plate with constant heat flux and variable suction have been analyzed by Sattar and Alam [3].

The momentum, heat, and mass transport on stretching sheet have several applications in polymer processing as well as in electrochemistry. The growing need for chemical reactions in chemical and hydrometallurgical industries requires the study of heat and mass transfer with chemical reaction. There are many transport processes that are governed by the combined action of buoyancy forces due to both thermal and mass diffusion in the presence of the chemical reaction. These processes are observed in nuclear reactor safety and combustion systems, solar collectors, as well as metallurgical and chemical engineering. Their other applications include solidification of binary alloys and crystal growth dispersion of dissolved materials or particulate water in flows, drying and dehydration operations in chemical and food processing plants, and combustion of atomized liquid fuels. The presence of foreign mass in water or air causes some kind of chemical reaction. Some foreign mass may be present either by itself or as mixtures with air or water. In many chemical engineering processes, a chemical reaction accurs between a foreign mass and the fluid in which the plate is moving. These processes take place in numerous industrial applications, for example, polymer production, manufacturing of ceramics or glassware, and food processing. From the point of applications, the effect of the first-order homogeneous chemical reaction of an unsteady flow past a vertical plate with the constant heat and mass transfer has been investigated by Das et al. [4]. The chemical reaction effects on an unsteady MHD free convection fluid flow past a semi infinite vertical plate embedded in a porous medium with heat absorption have been studied by Anand Rao et al. [5].

The heat and mass transfer occur simultaneously between the fluxes, the driving potentials are of more intricate nature. An energy flux can be generated not only by temperature gradients but by composition gradients. The energy flux caused by a composition is called Dufour or diffusion-thermo effect. Temperature gradients can also create mass fluxes, and this is the Soret or thermal-diffusion effect. Generally, the thermal-diffusion and the diffusion thermo effects are of smaller-order magnitude than the effects prescribed by Fourier’s or Fick’s laws and are often neglected in

heat and mass transfer processes. The thermal-diffusion effect, for instance, has been utilized for isotope separation and in mixture between gases with very light molecular weight (H_2,He) and of medium molecular weight (Nitrogen-air) the diffusion-thermo effect was found to be of a magnitude such that it cannot be neglected. The boundary layer-flows in the presence of Soret, and Dufour effects associated with the thermal diffusion and diffusion-thermo for the mixed convection have been analyzed by Kafoussias and Williams [6]. The Dufour and Soret effects on unsteady MHD free convection and mass transfer flow through a porous medium past an infinite vertical porous plate in a rotating system have been studied by Islam and Alam [7].

The interaction of buoyancy with thermal radiation has been increased greatly during the last decade due to its importance in many practical applications. The thermal radiation effect is important under many isothermal and nonisothermal situations. For industrial applications such as glass production, furnace design, space technology applications, cosmical flight aerodynamics rockets, and spacecraft re-entry aerothermodynamics which are operated under the higher temperature with radiation effects are significant. In view of this, the unsteady free convection interaction with thermal radiation in a boundary layer flow past a vertical porous plate has been investigated by Sattar and Kalim [8]. The above work has been investigated by Aydin and Kaya [9] with the extension of MHD mixed convection flow about a permeable vertical plate.

The Soret and Dufour effects have been found to influence the flow field in mixed convection boundary layer over a vertical surface embedded in a porous medium. The effect of thermal radiation, Hall currents, Soret and Dufour on MHD flow by mixed convection over a vertical surface in porous media has been studied by Shateyi et al. [10]. The effects of Soret, Dufour, chemical reaction, thermal radiation and volumetric heat generation/absorption on mixed convection stagnation point flow on an isothermal vertical plate in porous media has been analyzed by Olanrewaju and Gbadeyan [11]. The Micropolar fluid behaviors on unsteady MHD heat and mass transfer flow with constant heat and mass fluxes, joule heating and viscous dissipation has been investigated by Haque and Alam [12]. The effects of Soret and Dufour on unsteady MHD flow by mixed convection over a vertical surface in porous media with internal heat generation, chemical reaction and Hall current have been investigated by Aurangzaib and Shafie [13]. The finite difference solution of MHD mixed convection flow with heat generation and chemical reaction has been studied by Ahmed and Alam [14]. The effects of diffusion-thermo and thermal-diffusion on MHD visco-elastic fluid flow over a vertical plate have been investigated by Yasmin et al. [15] by using finite difference method. The chemically reacting ionized fluid flow through a vertical plate with inclined magnetic field in rotating system has been studied by Ahmed and Alam [16] by using

finite difference method. The finite difference solution of radiative MHD heat and mass transfer nanofluid flow past a horizontal plate in a rotating system has been investigated by Hasan et al. [17].

Hence our aim of this research is to extend the work of Ahmed and Alam [14]. The problem has been solved by finite difference method. The governing equations involved in this problem have been transformed into non-similar coupled partial differential equation by usual transformations. Finally, the comparison of the present results with the results of Aurangzaib and Shafie [13] has been shown graphically as well as tabular form.

2. Mathematical Formulation

A flow model of unsteady MHD mixed convective heat and mass transfer flow of an electrically conducting incompressible viscous fluid past an electrically nonconducting isothermal semi-infinite vertical porous plate with thermal diffusion and diffusion thermo effect are considered. The positive x coordinate is measured along the plate in the direction of fluid motion and the positive y coordinate is measured normal to the plate. The leading edge of the plate is taken as coincident with $z-$axis. Initially, it is considered that the plate as well as the fluid is at the same temperature $T(=T_\infty)$ and concentration level $C(=C_\infty)$. Also it is assumed that the fluid and the plate is at rest after that the plate is to be moving with a constant velocity U_∞ in its own plane. Instantaneously at time $t>0$, the temperature of the plate and spices concentration are raised to $T_w(>T_\infty)$ and $C_w(>C_\infty)$ respectively, which are there after maintained constant, where T_w, C_w are temperature and spices concentration at the wall and T_∞, C_∞ are the temperature and concentration of the species outside the plate respectively. The physical configuration of the problem is furnished in Fig. 1.

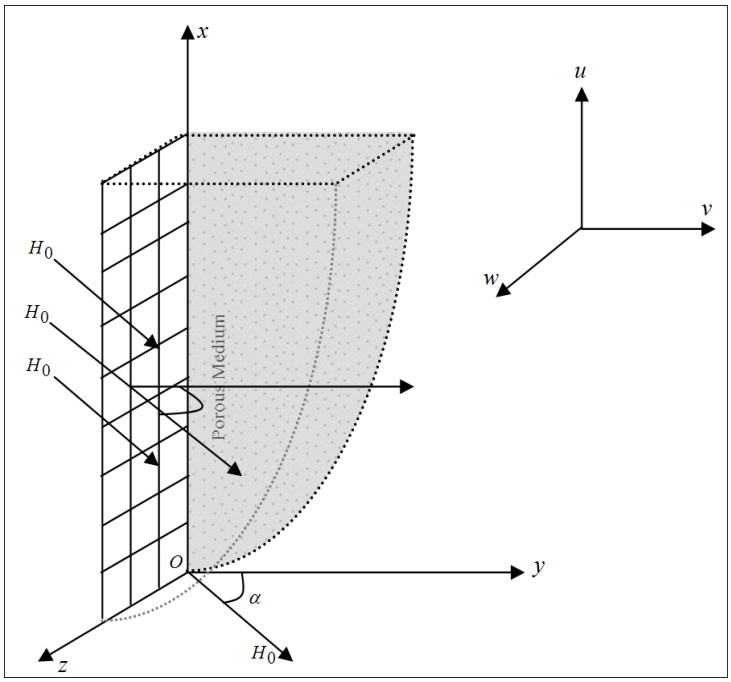

Fig.1. Geometrical configuration and coordinate system

A strong uniform magnetic field $\mathbf{H}$ can be taken as $\left(0, \lambda H_0, \sqrt{1-\lambda^2} H_0\right)$ where $\lambda = \cos\alpha$ is applied in a direction that makes an angle α with the normal to the considered plate. Thus if $\lambda = 1$ the imposed magnetic field is parallel to the $y-$axis and if $\lambda = 0$ then the magnetic field is parallel to the plate. The magnetic Reynolds number of the flow is taken to be small enough field and the magnetic field is negligible in comparison with applied magnetic field and the magnetic lines are fixed relative to the fluid. Using the relation $\nabla \cdot \mathbf{J} = 0$ for the current density $\mathbf{J} = \left(J_x, J_y, J_z\right)$ where $J_y = \text{constant}$. Since the plate is non conducting, $J_y = 0$ at the plate and hence zero everywhere. The generalized Ohm's law in the absence of electric field to the case of short circuit problem (Meyer [18] & Cowling [1]);

$$\mathbf{J} = \sigma\left(\mu_e \mathbf{q} \wedge \mathbf{H} + \frac{1}{ne} grad\, p_e\right) - \frac{\beta_e}{H_0}(\mathbf{J} \wedge \mathbf{H}) + \frac{\beta_i \beta_e}{H_0}(\mathbf{J} \wedge \mathbf{H}) \wedge \mathbf{H}$$

where $\sigma, \mu_e, n, e, p_e, \beta_e$ and β_i are the electric conductivity, the magnetic permeability, the number of density of electron, the electric charge, the electron pressure, Hall parameter, and Ion-slip parameter, respectively. If we neglect the electron pressure, we have

$$J_x = \frac{\sigma \mu_e H_0 \lambda}{\alpha_e \alpha_e' + \beta_e^2 \lambda^2}\left(u\beta_e \lambda - w\alpha_e'\right)$$

$$J_z = \frac{\sigma \mu_e H_0 \lambda}{\alpha_e \alpha_e' + \beta_e^2 \lambda^2}\left(w\beta_e \lambda + u\alpha_e\right)$$

where $\alpha_e = 1 + \beta_i \beta_e$ and $\alpha_e' = 1 + \beta_i \beta_e \lambda^2$

3. Governing Equations

Within the framework of the above-stated assumptions the generalized equations relevant to the unsteady free convective mass transfer problem are governed by the following system of coupled partial differential equations as;

Continuity equation

$$\frac{\partial u}{\partial x} + \frac{\partial v}{\partial y} = 0 \tag{1}$$

Momentum equations

$$\frac{\partial u}{\partial t} + u\frac{\partial u}{\partial x} + v\frac{\partial u}{\partial y} = \upsilon \frac{\partial^2 u}{\partial y^2} + gB_T\left(T - T_\infty\right) + gB_C\left(C - C_\infty\right)$$

$$- \frac{\sigma \mu_e^2 H_0^2 \lambda^2}{\rho\left(\alpha_e \alpha_e' + \beta_e^2 \lambda^2\right)}\left(w\beta_e \lambda + u\alpha_e\right) - \frac{\mu}{\rho k_1} u \tag{2}$$

$$\frac{\partial w}{\partial t} + u\frac{\partial w}{\partial x} + v\frac{\partial w}{\partial y} = \upsilon \frac{\partial^2 w}{\partial y^2} + \frac{\sigma \mu_e^2 H_0^2 \lambda^2}{\rho\left(\alpha_e \alpha_e' + \beta_e^2 \lambda^2\right)}\left(u\beta_e \lambda - w\alpha_e'\right) - \frac{\mu}{\rho k_1} w \tag{3}$$

Energy equation

$$\frac{\partial T}{\partial t} + u\frac{\partial T}{\partial x} + v\frac{\partial T}{\partial y} = \frac{\kappa}{\rho c_p}\frac{\partial^2 T}{\partial y^2} + \frac{Dk_t}{c_s c_p}\frac{\partial^2 C}{\partial y^2} + \frac{\sigma \mu_e H_0^2 \lambda^2}{\rho c_p\left(\alpha_e \alpha_e' + \beta_e^2 \lambda^2\right)^2}\left\{\left(w\beta_e \lambda + u\alpha_e\right)^2 + \left(u\beta_e \lambda - w\alpha_e'\right)^2\right\}$$

$$- \frac{1}{\rho c_p}\frac{\partial q_r}{\partial y} + \frac{Q}{\rho c_p}\left(T - T_\infty\right)^p \tag{4}$$

Concentration equation

$$\frac{\partial C}{\partial t} + u\frac{\partial C}{\partial x} + v\frac{\partial C}{\partial y} = D\frac{\partial^2 C}{\partial y^2} + \frac{Dk_t}{T_m}\frac{\partial^2 T}{\partial y^2} - k_0\left(C - C_\infty\right)^q \tag{5}$$

with the corresponding boundary conditions are;

$$u = U_\infty,\ w = 0,\ T = T_w,\ C = C_w \quad \text{at } y = 0 \tag{6}$$

$$u = 0,\ w = 0,\ T \to T_\infty,\ C \to C_\infty \quad \text{as } y \to \infty$$

where u, v and w are the x, y and z components of velocity vector, υ is the kinematic coefficient viscosity, μ is the fluid viscosity, ρ is the density of the fluid, κ is the thermal conductivity, c_p is the specific heat at the constant pressure , k_0 is the rate of chemical reaction and D is the coefficient of mass diffusivity, k_t is the thermal diffusion ratio, c_s is the concentration

susceptibility, respectively. Here p and q are considered as positive constant. The radiative heat flux q_r is described by the Rosseland approximation such that $q_r = -\frac{4\sigma^*}{3k^*}\frac{\partial T^4}{\partial y}$, where σ^* and k^* are the Stefan-Boltzman constant and the mean absorption coefficient, respectively. If the temperature difference within the flow are sufficiently small so that the T^4 can be expressed as a linear function after using Taylor series to expand T^4 about the free stream temperature T_∞ and neglecting higher-order terms. This result in the following approximation: $T^4 \approx 4T_\infty^3 T - 3T_\infty^4$.

To obtain the governing equations and the boundary condition in dimension less form, the following non-dimensional quantities are introduced as; $X = \frac{xU_\infty}{\upsilon}$, $Y = \frac{yU_\infty}{\upsilon}$, $U = \frac{u}{U_\infty}$, $V = \frac{v}{U_\infty}$, $W = \frac{w}{U_\infty}$, $\tau = \frac{tU_\infty^2}{\upsilon}$, $\overline{T} = \frac{T - T_\infty}{T_w - T_\infty}$ and $\overline{C} = \frac{C - C_\infty}{C_w - C_\infty}$

Substituting the above dimensionless variables in equations (1)-(5) and corresponding boundary conditions (6) are;

$$\frac{\partial U}{\partial X} + \frac{\partial V}{\partial Y} = 0 \tag{7}$$

$$\frac{\partial U}{\partial \tau} + U\frac{\partial U}{\partial X} + V\frac{\partial U}{\partial Y} = \frac{\partial^2 U}{\partial Y^2} + G_r\overline{T} + G_m\overline{C} - \frac{M}{\left(\alpha_e\alpha_e' + \beta_e^2\lambda^2\right)}\left(W\beta_e\lambda + U\alpha_e\right) - KU \tag{8}$$

$$\frac{\partial W}{\partial \tau} + U\frac{\partial W}{\partial X} + V\frac{\partial W}{\partial Y} = \frac{\partial^2 W}{\partial Y^2} + \frac{M}{\left(\alpha_e\alpha_e' + \beta_e^2\lambda^2\right)}\left(U\beta_e\lambda - W\alpha_e'\right) - KW \tag{9}$$

$$\frac{\partial \overline{T}}{\partial \tau} + U\frac{\partial \overline{T}}{\partial X} + V\frac{\partial \overline{T}}{\partial Y} = \left(\frac{1+R}{P_r}\right)\frac{\partial^2 \overline{T}}{\partial Y^2} + D_u\frac{\partial^2 \overline{C}}{\partial Y^2} + \frac{ME_c}{\left(\alpha_e\alpha_e' + \beta_e^2\lambda^2\right)^2}\left\{\left(W\beta_e\lambda + U\alpha_e\right)^2 + \left(U\beta_e\lambda - W\alpha_e'\right)^2\right\} + \beta\overline{T}^{\,p} \tag{10}$$

$$\frac{\partial \overline{C}}{\partial \tau} + U\frac{\partial \overline{C}}{\partial X} + V\frac{\partial \overline{C}}{\partial Y} = \frac{1}{S_c}\frac{\partial^2 \overline{C}}{\partial Y^2} + S_r\frac{\partial^2 \overline{T}}{\partial Y^2} - \gamma\overline{C}^{\,q} \tag{11}$$

boundary conditions are;

$$U = 1,\ W = 0,\ \overline{T} = 1,\ \overline{C} = 1 \text{ at } Y = 0 \tag{12}$$

$$U = 0,\ W = 0,\ \overline{T} = 0,\ \overline{C} = 0 \text{ as } Y \to \infty,$$

where τ represents the dimensionless time, Y is the dimensionless Cartesian coordinate, U and W are the dimensionless primary velocity and secondary velocity, $\overline{T}$ is the dimensionless temperature,

$\overline{C}$ is the dimensionless concentration, $G_r = \frac{gB_T(T_w - T_\infty)\upsilon}{U_\infty^3}$ (Grashof Number), $G_m = \frac{gB_C(C_w - C_\infty)\upsilon}{U_\infty^3}$ (Modified Grashof Number), $K = \frac{\mu\upsilon}{\rho k_1 U_\infty^2}$ (Permeability of the porous medium), $M = \frac{\sigma B_0^2 \upsilon}{\rho U_\infty^2}$ (Magnetic Parameter), $R = \frac{16\sigma^* T_\infty^3}{3k^*\kappa}$ (Radiation Parameter), $P_r = \frac{\rho c_p \upsilon}{\kappa}$ (Prandtl Number), $D_u = \frac{Dk_t}{\upsilon c_s c_p}\frac{(C_w - C_\infty)}{(T_w - T_\infty)}$ (Dufour Number), $E_c = \frac{U_\infty^2}{c_p(T_w - T_\infty)}$ (Eckert Number), $\beta = \frac{Q\upsilon(T_w - T_\infty)^{p-1}}{\rho c_p U_\infty^2}$ (Heat Generation or Absorption Parameter), $S_c = \frac{\upsilon}{D}$ (Schmidt Number), $S_r = \frac{Dk_T}{\upsilon T_m}\frac{(T_w - T_\infty)}{(C_w - C_\infty)}$ (Soret Number) and $\gamma = \frac{k_0\upsilon(C_w - C_\infty)^{q-1}}{U_\infty^2}$ (Chemical Reaction Parameter).

4. Numerical Solutions

To solve the governing dimensionless partial differential equations with the associated initial and boundary conditions, the finite difference method has been used. To obtain the difference equations the region of the flow is divided into a grid of lines parallel to X and Y axes where X-axis is taken along the plate and Y-axis is normal to the plate.

Here the plate of height $X_{\max}(=100)$ is considered i.e. X varies from 0 to 100 and assumed $Y_{\max}(=35)$ as corresponding to $Y \to \infty$ i.e. Y varies from 0 to 35. There are $m(=200)$ and $n(=200)$ grid spacing in the X and Y directions respectively as shown Fig. 2. It is assumed that ΔX, ΔY are constant mesh size along X and Y directions respectively and taken as follows, $\Delta X = 0.5(0 \le X \le 100)$ and $\Delta Y = 0.175(0 \le Y \le 35)$ with the smaller time-step, $\Delta\tau = 0.005$.

Let $U', W', \overline{T}'$ and $\overline{C}'$ denote the values of $U, W, \overline{T}$ and $\overline{C}$ ate the end of a time-step respectively. Using the finite difference approximation, the following appropriate set of finite difference equations are obtained as;

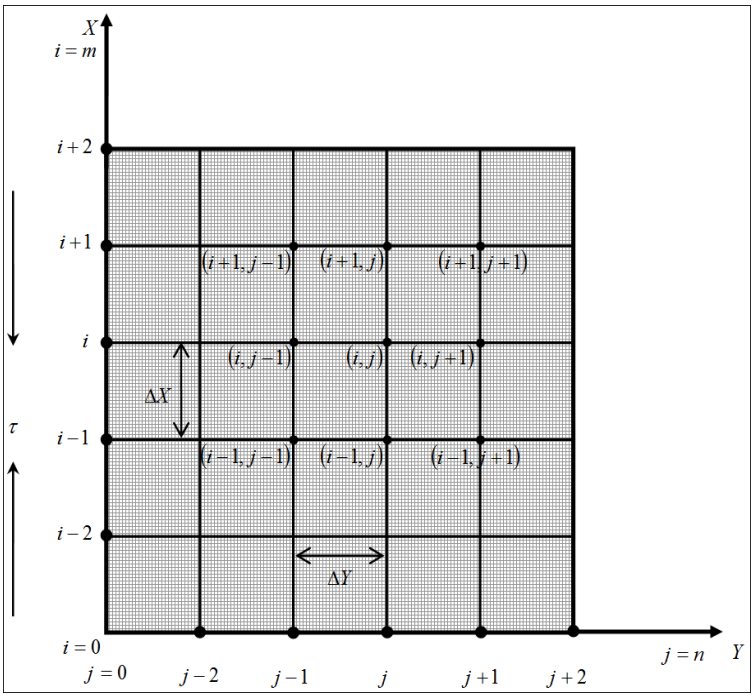

Fig. 2. Finite difference system grid

$$\frac{U'_{i,j}-U'_{i-1,j}}{\Delta X}+\frac{V_{i,j}-V_{i-1,j}}{\Delta Y}=0 \tag{13}$$

$$\frac{U'_{i,j}-U_{i,j}}{\Delta\tau}+U_{i,j}\frac{U_{i,j}-U_{i-1,j}}{\Delta X}+V_{i,j}\frac{U_{i,j+1}-U_{i,j}}{\Delta Y}=\frac{U_{i,j+1}-2U_{i,j}+U_{i,j-1}}{(\Delta Y)^2}+G_r\overline{T}_{i,j}+G_m\overline{C}_{i,j}$$
$$-\frac{M}{\left(\alpha_e\alpha'_e+\beta_e^2\lambda^2\right)}\left(W_{i,j}\beta_e\lambda+U_{i,j}\alpha_e\right)-KU_{i,j} \tag{14}$$

$$\frac{W'_{i,j}-W_{i,j}}{\Delta\tau}+U_{i,j}\frac{W_{i,j}-W_{i-1,j}}{\Delta X}+V_{i,j}\frac{W_{i,j+1}-W_{i,j}}{\Delta Y}=\frac{W_{i,j+1}-2W_{i,j}+W_{i,j-1}}{(\Delta Y)^2}-KW_{i,j}$$
$$+\frac{M}{\left(\alpha_e\alpha'_e+\beta_e^2\lambda^2\right)}\left(U_{i,j}\beta_e\lambda-W_{i,j}\alpha'_e\right) \tag{15}$$

$$\frac{\overline{T}'_{i,j}-\overline{T}_{i,j}}{\Delta\tau}+U_{i,j}\frac{\overline{T}_{i,j}-\overline{T}_{i-1,j}}{\Delta X}+V_{i,j}\frac{\overline{T}_{i,j+1}-\overline{T}_{i,j}}{\Delta Y}=\left(\frac{1+R}{P_r}\right)\frac{\overline{T}_{i,j+1}-2\overline{T}_{i,j}+\overline{T}_{i,j-1}}{(\Delta Y)^2}+D_u\frac{\overline{C}_{i,j+1}-2\overline{C}_{i,j}+\overline{C}_{i,j-1}}{(\Delta Y)^2}$$
$$+\frac{ME_c}{\left(\alpha_e\alpha'_e+\beta_e^2\lambda^2\right)^2}\left\{\left(W_{i,j}\beta_e\lambda+U_{i,j}\alpha_e\right)^2+\left(U_{i,j}\beta_e\lambda-W_{i,j}\alpha'_e\right)^2\right\}+\beta\left(\overline{T}_{i,j}\right)^p \tag{16}$$

$$\frac{\overline{C}'_{i,j}-\overline{C}_{i,j}}{\Delta\tau}+U_{i,j}\frac{\overline{C}_{i,j}-\overline{C}_{i-1,j}}{\Delta X}+V_{i,j}\frac{\overline{C}_{i,j+1}-\overline{C}_{i,j}}{\Delta Y}=\frac{1}{S_c}\frac{\overline{C}_{i,j+1}-2\overline{C}_{i,j}+\overline{C}_{i,j-1}}{(\Delta Y)^2}$$
$$+S_r\frac{\overline{T}_{i,j+1}-2\overline{T}_{i,j}+\overline{T}_{i,j-1}}{(\Delta Y)^2} \tag{17}$$

with the boundary conditions,

$$U_{i,0}^{n}=1,\ W_{i,0}^{n}=0,\ \overline{T}_{i,0}^{n}=1,\ \overline{C}_{i,0}^{n}=1 \tag{18}$$

$$U_{i,L}^{n}=1,\ W_{i,L}^{n}=0,\ \overline{T}_{i,L}^{n}=1,\ \overline{C}_{i,L}^{n}=1 \text{ where } L\to\infty$$

Here the subscript i and j designates the grid points with X and Y coordinates respectively and the superscript n represents a value of time, $\tau=n\Delta\tau$ where $n=0,1,2,\ldots\ldots$. The primary velocity (U), secondary velocity (W), temperature $(\overline{T})$ and concentration $(\overline{C})$ distributions at all interior nodal points may be computed by successive applications of the above finite difference equations. The numerical values of the local shear stresses, local Nusselt number and local Sherwood number are evaluated by Five-point approximate formula for the derivatives and then the average Shear Stress, Current density, Nusselt number and Sherwood number are calculated by the use of the Simpson's $\frac{1}{3}$ integration formula. The stability conditions and the convergence criteria are not shown for brevity.

5. Results and Discussion

In order to investigate the physical situation of the problem, the numerical values and graphs of primary velocity (U), secondary velocity (W), temperature $(\overline{T})$ and concentration $(\overline{C})$ distributions within the boundary layer have been computed for different values Suction parameter (S), Permeability of the porous medium (K), Magnetic parameter (M), Hall parameter (β_e), Ion-slip parameter (β_i), Radiation parameter (R), Prandtl number (P_r), Dufour number (D_u), Eckert Number (E_c), Heat Generation or Absorption parameter (β), Schmidt number (S_c), Soret number (S_r), Chemical reaction parameter (γ) with the help of a computer programming language Compaq Visual Fortran 6.6a and Tecplot 7. These computed numerical results have been shown graphically. To obtain the steady-state solutions, the computation has been carried out up to $\tau=80$. It is observed that the numerical values of $U, W, \overline{T}$ and $\overline{C}$ however, show little changes after $\tau=50$. Hence at $\tau=50$, the solutions of all variables are steady-state solutions.

To observe the physical situation of the problem, the steady-state solutions have been illustrated in Figs. 4-28 when $p=2$ and $q=2$. The primary velocities, secondary velocities and temperature distributions have been displayed for various values of Radiation parameter (R) and Dufour number (D_u) respectively illustrated in Figs. 4-6. These results show that the primary

velocities, secondary velocities and temperature distributions increase with the increase of Radiation parameter and Dufour number. The effects of Magnetic parameter (M) on primary and secondary velocities have been respectively illustrated in Figs. 7 and 8. These results show that the primary velocities decrease and secondary velocities increase with the increase of Magnetic parameter. The primary velocities have been displayed for various values of Eckert number (E_c) in Fig. 9. These results show that the primary velocities increase with the increase of Eckert number.

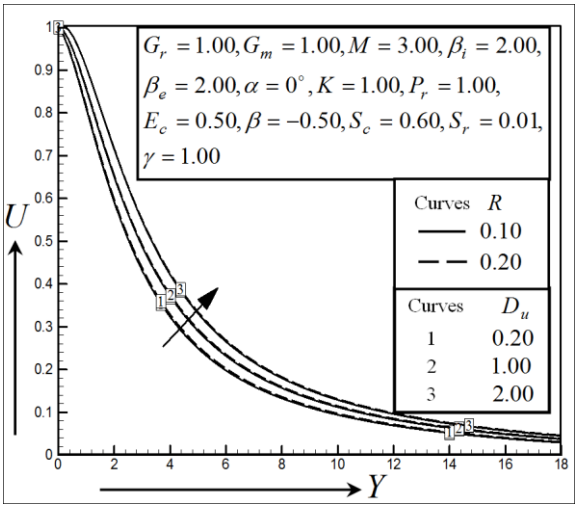

Fig. 4. Illustration of primary velocity profiles for various values of Radiation parameter, R and Dufour number, D_u.

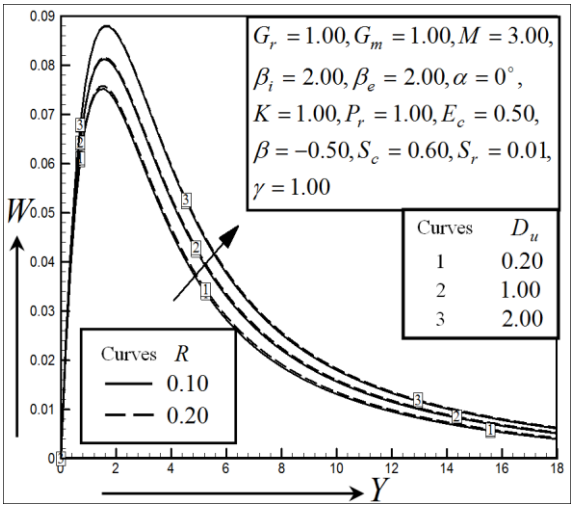

Fig. 5. Illustration of secondary velocity profiles for various values of Radiation parameter, R and Dufour number, D_u.

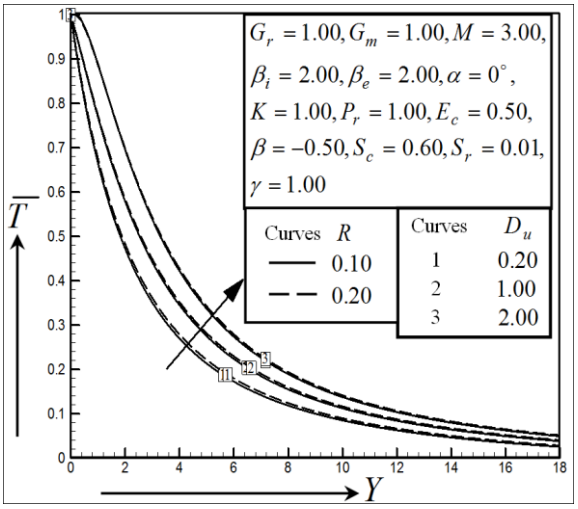

Fig. 6. Illustration of temperature profiles for various values of Radiation parameter, R and Dufour number, D_u.

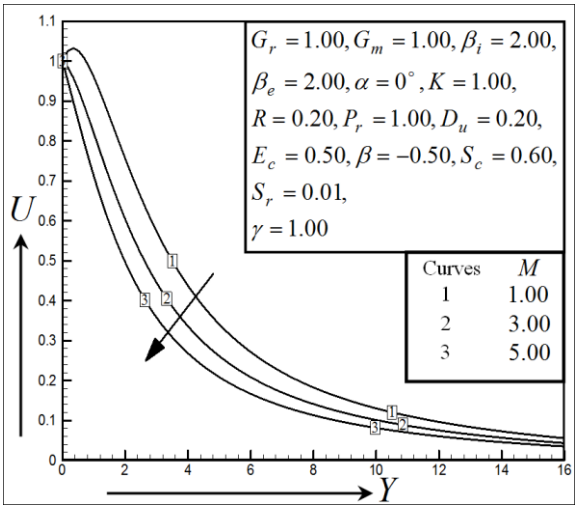

Fig. 7. Illustration of primary velocity profiles for various values of Magnetic parameter, M.

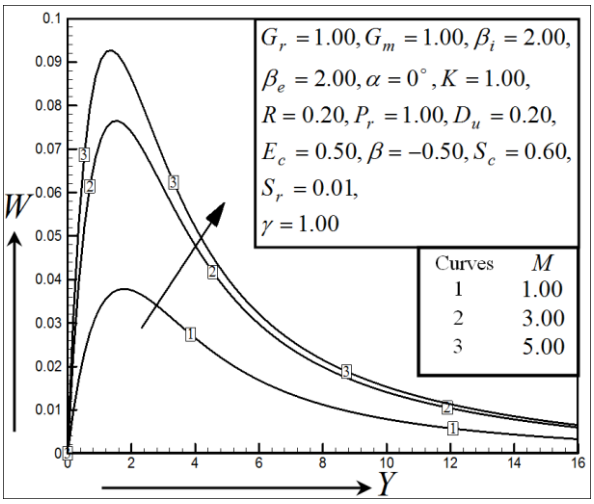

Fig. 8. Illustration of secondary velocity profiles for various values of Magnetic parameter, M .

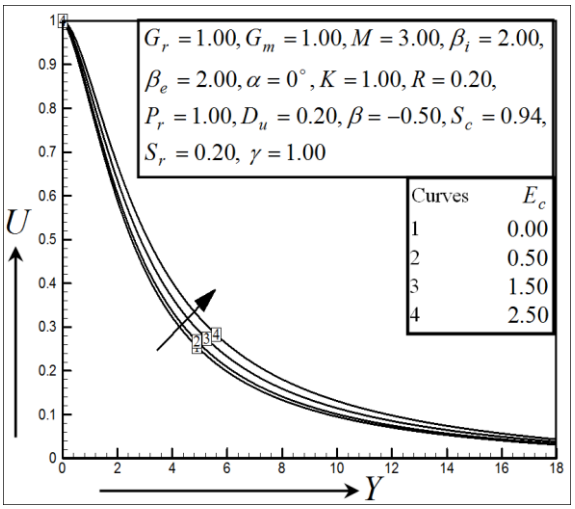

Fig. 9. Illustration of primary velocity profiles for various values of Eckert number, E_c.

The secondary velocities and temperature distributions have been displayed for various values of Eckert number (E_c) respectively illustrated in Figs. 10 and 11. These results show that the secondary velocities and temperature distributions increase with the increase of Eckert number. The primary velocities and secondary velocities have been shown in Figs. 12 and 13 for various values of chemical reaction parameter (γ) with two values of Schimdt number $S_c = 0.60$ (water vapor) and $S_c = 0.94$ (carbon dioxide) respectively. It is noted that the primary velocities and secondary velocities decrease with the increase of chemical reaction parameter (γ), where $\gamma < 0$ and $\gamma > 0$ are treated as genarative and destructive chemical reaction respectively. The primary velocities and secondary velocities also decrease with the increase of Schimdt number leads to thining of the concentration boundary layers.

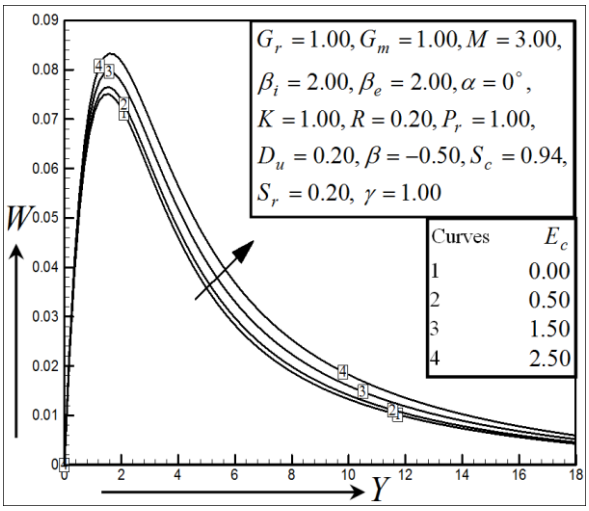

Fig. 10. Illustration of secondary velocity profiles for various values of Eckert number, E_c.

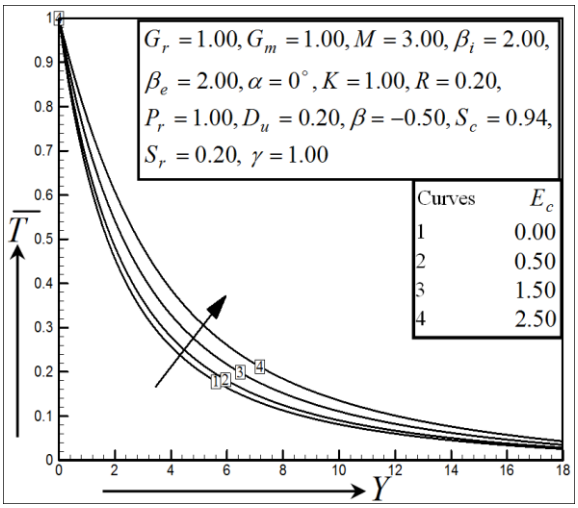

Fig. 11. Illustration of temperature profiles for various values of Eckert number, E_c.

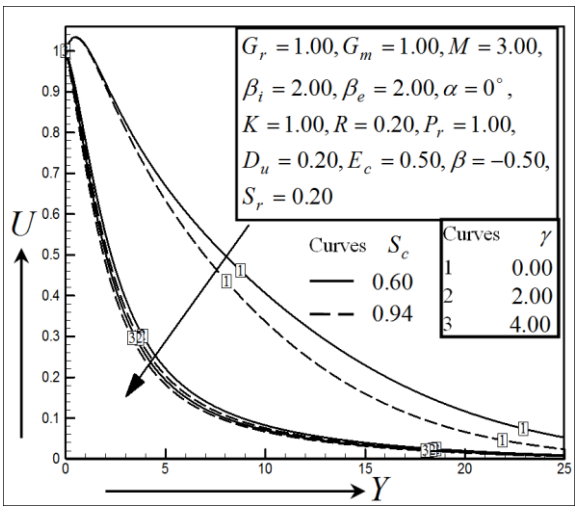

Fig. 12. Illustration of primary velocity profiles for various values of Schimit number, S_c and Chemical reaction parameter, γ.

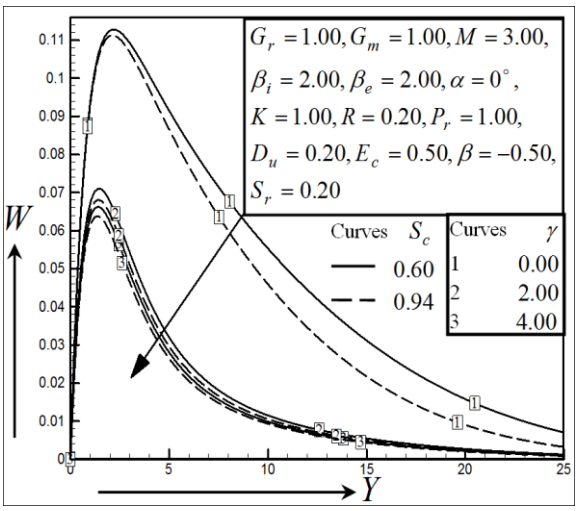

Fig. 13. Illustration of secondary velocity profiles for various values of Schimit number, S_c and Chemical reaction parameter, γ.

The concentrations profiles have been shown in Fig. 14 for various values of chemical reaction parameter (γ) with two values of Schimdt number $S_c = 0.60$ (water vapor) and $S_c = 0.94$ (carbon dioxide) respectively. It is noted that the fluid concentrations decrease with the increase of chemical reaction parameter and Schimdt number leads to thining of the concentration boundary layers. Figs. 15-17 display the primary velocities, secondary velocities and temperature distributions for several values of heat generation or absorption parameter (β) and Prandtl number (P_r). It is noted that the

primary velocities, secondary velocities and fluid temperature increase with the increase of heat generation or absorption parameter (β). The primary velocities, secondary velocities and fluid temperautre decrease with the increase of Prandtl number. This is consistent with the well known fact that the thermal boundary layer thickness decreases with the increase of Prandlt number.

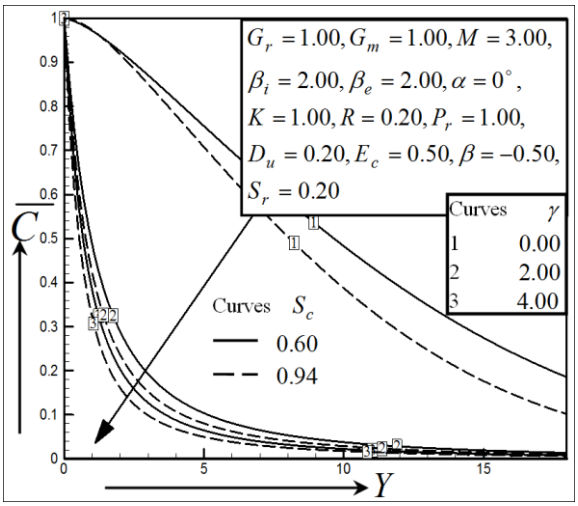

Fig. 14. Illustration of concentration profiles for various values of Schimit number, S_c and Chemical reaction parameter, γ.

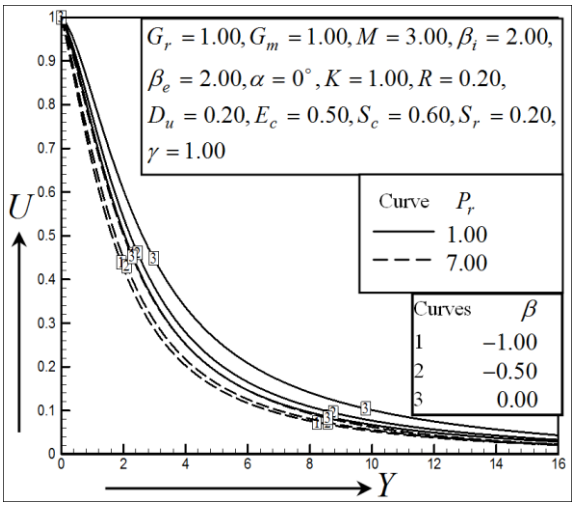

Fig. 15. Illustration of primary velocity profiles for various values of Prandtl number, P_r and Heat genaration or absorption parameter, β.

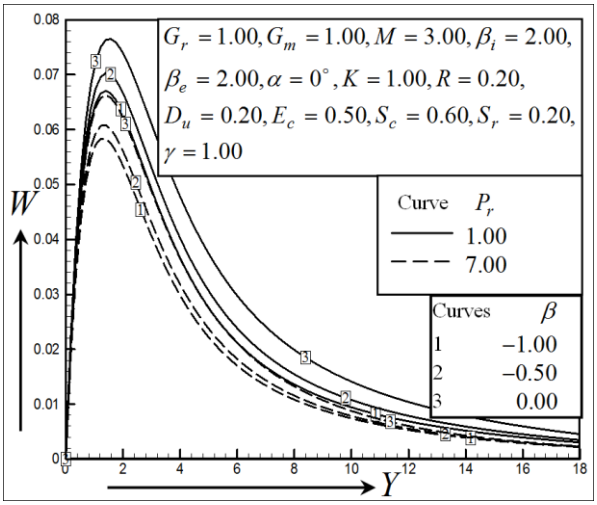

Fig. 16. Illustration of secondary velocity profiles for various values of Prandtl number, P_r and Heat genaration or absorption parameter, β.

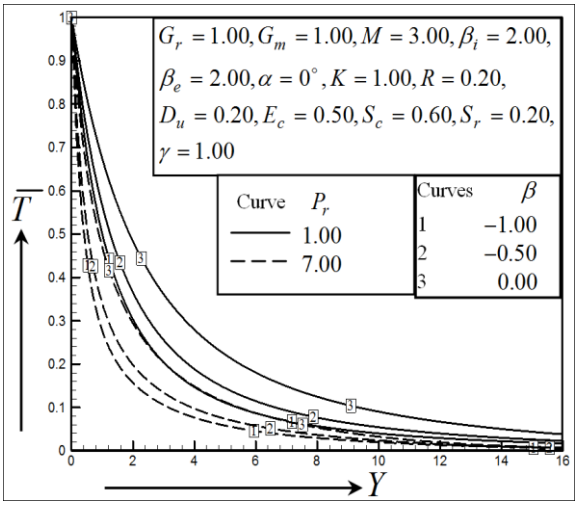

Fig. 17. Illustration of temperature profiles for various values of Prandtl number, P_r and Heat genaration or absorption parameter, β.

Figs. 18 & 19 and 20 & 21 show the primary and secondary velocities for various values of Hall parameter (β_e) and Ion-slip parameter (β_i) respectively. These results show that the primary velocities increase and the secondary velocities decrease with the increase of both Hall parameter and Ion-slip parameter.

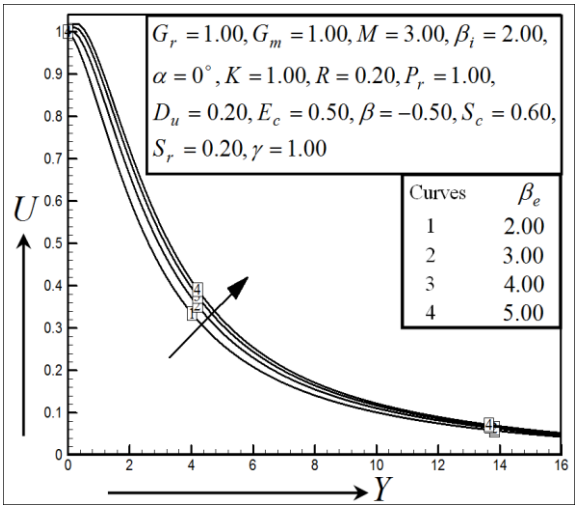

Fig. 18. Illustration of primary velocity profiles for various values of Hall parameter, β_e.

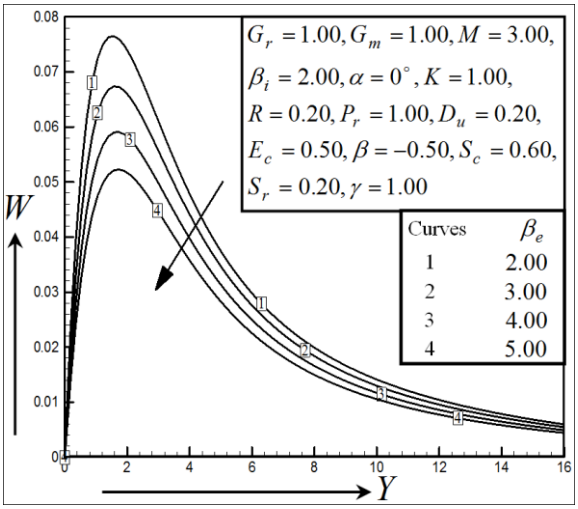

Fig. 19. Illustration of secondary velocity profiles for various values of Hall parameter, β_e.

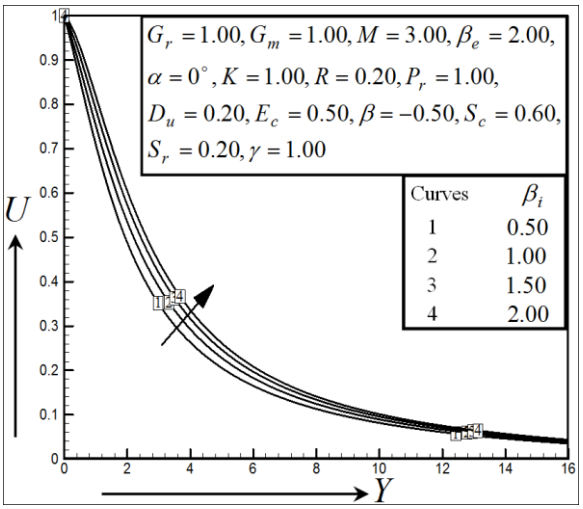

Fig. 20. Illustration of primary velocity profiles for various values of Ion-slip parameter, β_i.

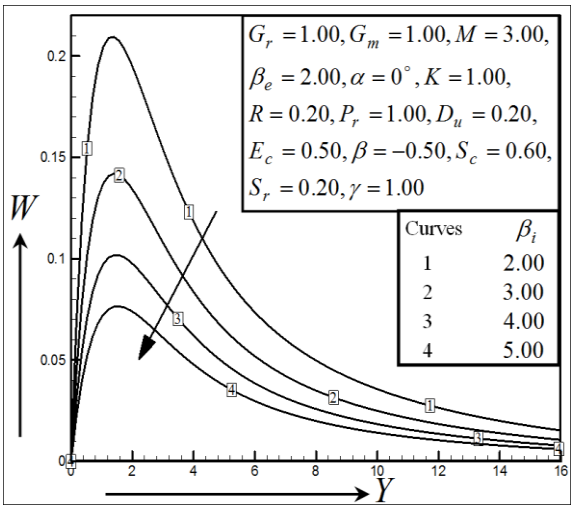

Fig. 21. Illustration of secondary velocity profiles for various values of Ion-slip parameter, β_i.

Figs. 22 and 23 show the primary and secondary velocities for various values of Permeability of the porous medium (K) respectively. These results show that the primary velocities and the

secondary velocities decrease with the increase of Permeability of the porous medium. The primary velocities, secondary velocities and concentration distributions have been respectively illustrated in Figs. 24-26 for various values of Soret number (S_r). These results show that the primary velocities, secondary velocities and concentration distributions increase with the increase of Soret number. The effects of α on primary and secondary velocity have been respectively illustrated in Figs. 27 and 28. These results show that the primary velocities decrease and the secondary velocities increase with the increase α.

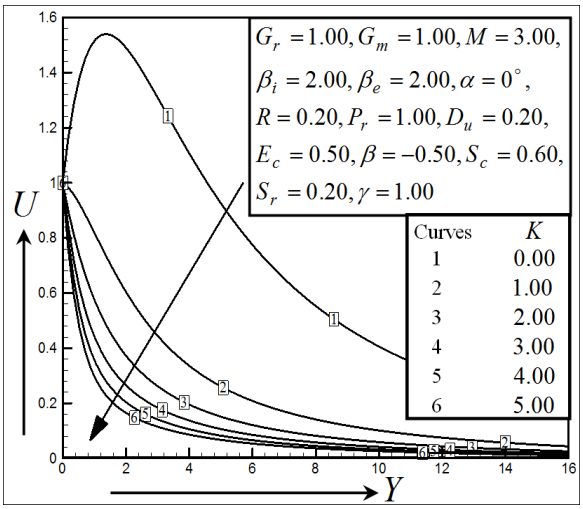

Fig. 22. Illustration of primary velocity profiles for various values of Permeability of the porous media, K.

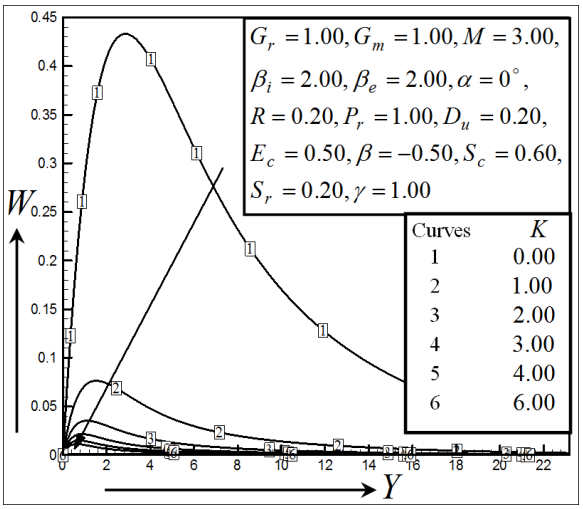

Fig. 23. Illustration of secondary velocity profiles for various values of Permeability of the porous media, K.

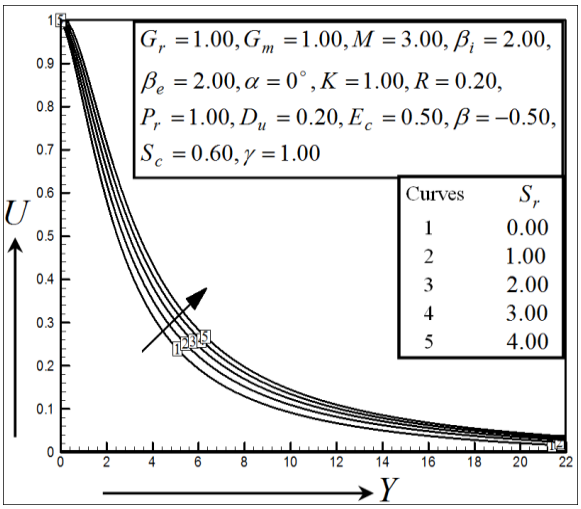

Fig. 24. Illustration of primary velocity profiles for various values of Soret number, S_r.

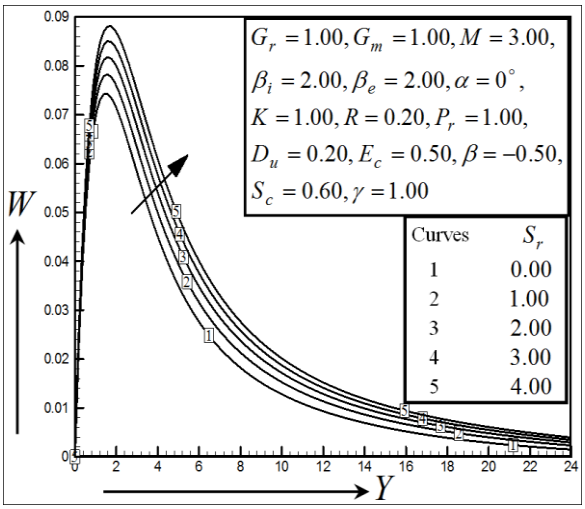

Fig. 25. Illustration of secondary velocity profiles for various values of Soret number, S_r.

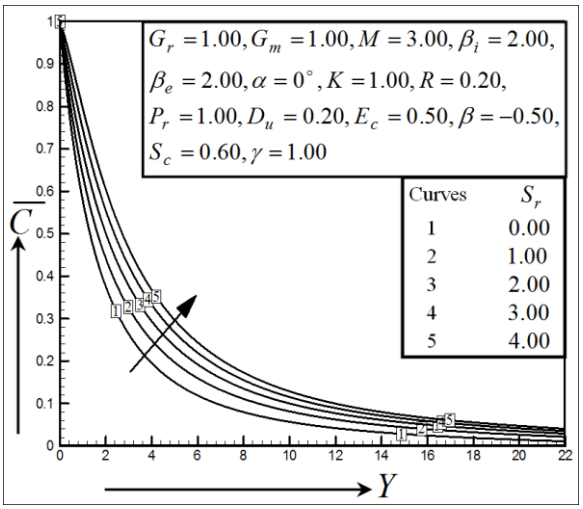

Fig. 26. Illustration of concentration profiles for various values of Soret number, S_r.

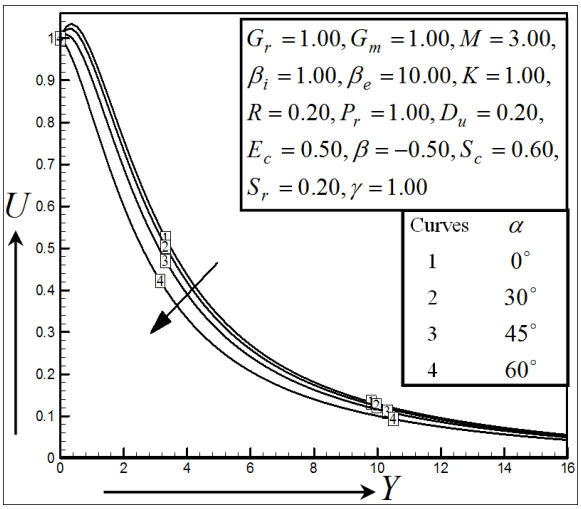

Fig. 27. Illustration of primary velocity profiles for various values of α.

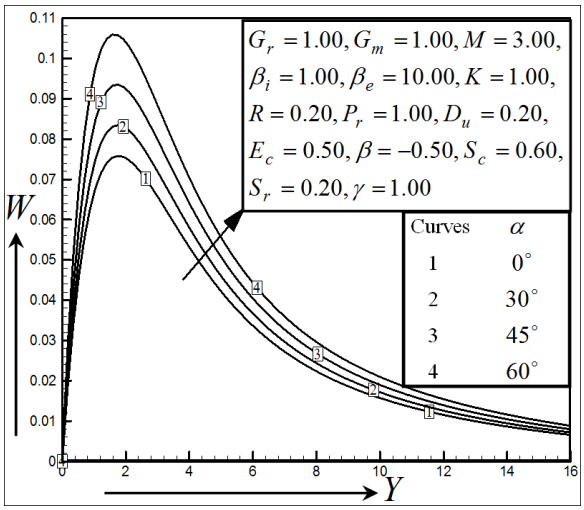

Fig. 28. Illustration of secondary velocity profiles for various values of α.

Finally, a qualitative comparison of the present steady-state results with the published results (Aurangzaib and Shafie [13]) is presented in table 1. The accuracy of the present results is qualitatively good in case of all the flow parameters.

Table 1. Qualitative comparison of the present results with the previous results

Increased Parameter	Previous results given by Aurangzaib and Shafie [13]				Present results			
	$f'(\eta)$	$h(\eta)$	$\theta(\eta)$	$\phi(\eta)$	U	W	$\overline{T}$	$\overline{C}$
R			Inc.		Inc.	Inc.	Inc.	
D_u	Inc.	Inc.	Inc.		Inc.	Inc.	Inc.	
M					Dec.	Inc.		
E_c					Inc.	Inc.	Inc.	
S_c	Dec.	Dec.		Dec.	Dec.	Dec.		Dec.
γ	Dec.	Dec.		Dec.	Dec.	Dec.		Dec.
P_r			Dec.		Dec.	Dec.	Dec.	
β			Inc.		Inc.	Inc.	Inc.	
β_e					Inc.	Dec.		
β_i					Inc.	Dec.		
K	Dec.	Dec.			Dec.	Dec.		
S_r	Inc.	Inc.		Inc.	Inc.	Inc.		Inc.
α					Inc.	Dec.		

Conclusions

In this study, the finite difference solution of unsteady ionized fluid flow on Impulsive vertical plate with inclined magnetic field in the presence of heat generation, chemical reaction and thermal radiation for $p \leq 2$ and $q \leq 2$ is investigeted. Important findings of this investigation are given below,

1. The primary velocity, secondary velocity and fluid temperature increase with the increase of Radiation parameter, Dufour number, Eckert number, and Heat genaration or absorption parameter and reverse effects with the increse of Prandtl number.

2. The primary velocities decrease and secondary velocities increase with the increase of Magnetic parameter & α and reverse effects with the increse of Hall parameter & Ion-slip parameter.

3. The primary velocities, secondary velocities and fluid concentration decrease with the increase of chemical reaction parameter & Schimidt number and reverse effects with the increse of Soret number.

4. The primary and secondary velocities decrease with the increase Permeability of the Porous medium.

It is hoped that the findings of this investigation may be useful for the study of movement of oil or gas, producing electricity**;** these results are also of great interest in geophysics, astrophysics and fluid engineering. It i8s also important in plasma studies as well as in power engineering, geothermal energy extractions, generators and boundary layer control in the field of aerodynamics.

As the basis of many scientific and engineering applications, for studying more complex problems involving the flow of electrically conducting fluids, it is assumed that the present investigation of unsteady ionized fluid flow on impulsive vertical plate with inclined magnetic field in the presence of heat generation, chemical reaction and thermal radiation can be utilized.

References

1. Cowling, T. G., "Magnetohydrodynamics", Interscience Publications, *New York*, 1957.
2. Ram, P. C., "Unsteady MHD free-convective flow through a porous medium with Hall currents", *Astrophysics and Space Science*, Vol. 149, pp. 171-174. 1988.
3. Sattar, M. A., and Alam, M. M., "MHD free convective heat and mass transfer with Hall current and constant heat flux through a porous medium", *Indian Journal of Applied Mathematics*, Vol. 26(2), pp. 157-167, 1995.
4. Das, U. N., Dekha, R., and Soungalgekar, V. M., "Effects on mass transfer on flow past an impulsive started infinite vertical plate with constant heat flux and chemical reaction", *Fursuhungim Ingenieurwesen*, Vol. 60, pp. 284-287, 1994.
5. Anand Rao, J., Sivaiah, S., and Srinivasa Raju, R., "Chemical reaction effects on an unsteady MHD free convection fluid flow past a semi-infinite vertical plate embedded in a porous medium with heat absorption", *Journal of Applied Fluid Mechanics*, Vol. 5(3), pp. 63-70, 2012.
6. Kafoussias, N. G., & Williams, E. W., "Thermal-diffusion and diffusion-thermo effects on mixed free-forced convective and mass transfer boundary layer flow with temperature dependent viscosity", *International Journal of Engineering Science*, Vol**.** 33(9), pp. 1369-1384, 1995.
7. Islam, N., & Alam, M. M., "The Dufour and Soret effects on unsteady MHD free convection and mass transfer flow through a porous medium past an infinite vertical porous plate in a roatating system", *Bangladesh Journal of Scientific and Industrial Research*, Vol. 43(2), pp. 159-172, 2008.
8. Sattar, M. A., and Kalim, H., "Unsteady free-convection interaction with thermal radiation in a boundary layer flow past a vertical porous plate", *Journal of Mathematical Physics*, Vol. 30(1), pp. 25-37, 1996.
9. Aydin, O., and Kaya, A., "Radiation effect on MHD mixed convection flow about a permeable vertical plate", *Heat Mass Transfer*, Vol. 45, pp.239-246, 2008.
10. Shateyi, S., Mosta, S. S. and Sibanda, P., "The effects of thermal radiation, Hall currents, soret doufor on MHD flow by mixed convection over a vertical surface in porous media", *Mathematical Problems in Engineering*, Article ID 627475, 2010.
11. Olanrewaju, P.O. and Gbadeyan, J.A., " Effects of Soret, Dufour, chemical reaction, thermal radiation and volumentric heat generation/absorption on mixed convection stagnation point flow on an Iso-thermal vertical plate in porous media", *Pacific Journal of Science and Technology*, Vol. 11(2), pp. 1-12, 2010.

12. Haque M. Z. and Alam, M. M., "Micropolar fluid behaviours on unsteady MHD heat and mass transfer flow with constant heat and mass fluxes, joule heating and viscous dissipation", *AMSE Journals, Modeling B,Mechanics and Thermics*, Vol. 80, N^0 2, pp. 1-25, 2011.
13. Aurangzaib and Sharidan Shafie, "Effects of Soret and Dufour on unsteady MHD flow by mixed convection over a vertical surface in porous media with internal heat generation, chemical reaction and Hall current", *Canadian Journal on Science and Engineering Mathematics,* Vol. 2(4), pp. 153-162, 2011.
14. Ahmed, T., and Alam, M. M., "Finite difference solution of MHD mixed convection flow with heat generation and chemical reaction, *Procedia of Engineering*, Vol. 56, pp. 149-156, 2013.
15. Yasmin, D., Ahmed, T., Anika, N. N., Hasan, M. M., and Alam, M. M., " Diffusion-thermo and Thermal-diffusion effects on MHD visco-elastic fluid flow over a vertical plate", *Journal of Applied Fluid Mechanics*, Vol. 7(3), 447-458, 2014.
16. Ahmed, T., and Alam, M. M., "Chemically reacting ionized fluid flow through a vertical plate with inclined magnetic field in rotating system", *Procedia of Engineering*, Vol. 90, pp. 301-307, 2014.
17. Hasan, M. M., Ahmed, T., and Alam, M. M., " Radiative MHD heat and mass transfer nanofluid flow past a horizontal plate in a rotating system", *Procedia Engineering*, Vol. 90, pp. 478-484, 2014.
18. Meyer, .R. C., "On reducing aerodynamic heat transfer rates by magneto-hydrodynamic techniques", *Journal of Aerospace Science,* Vol. 25, pp. 561, 1958.